

# DOUBLE-STAGE ORC SYSTEM BASED ON VARIOUS TEMPERATURE WASTE HEAT SOURCES OF THE NEGATIVE CO<sub>2</sub> POWER PLANT

Kamil Stasiak\*, Paweł Ziółkowski, Dariusz Mikielewicz

*Gdańsk University of Technology, Faculty of Mechanical Engineering and Ship Technology, Institute of Energy, 11/12 Gabriela Narutowicza Street, 80-233 Gdańsk, Poland*

\*Corresponding Author: [kamil.stasiak@pg.edu.pl](mailto:kamil.stasiak@pg.edu.pl)

## ABSTRACT

Analysed is the modification of the thermodynamic cycle with the negative CO<sub>2</sub> power plant concept by its combination with the organic Rankine cycle. The analysed power plant operates on a gas produced from the gasification of sewage sludge. The negative emission term comes from the aggregated CO<sub>2</sub> balance resulting from the capture of the CO<sub>2</sub>, while the sewage sludge is one of the inevitable environmental sources of CO<sub>2</sub> to be avoided. In short, the principle of this power plant is to produce electrical power by converting sewage sludge fuel as the substrate to CO<sub>2</sub> as a product, which is an intricate process in-between, with many opportunities for waste heat recovery. There are four main sources of waste heat in such a system. One is the drying process of the producer gas, which must be properly cooled from the high temperature after gasification to the temperature at which no moisture is present in the gas. In the wet combustion chamber, the syngas is oxy-combusted under high temperatures with water injection to control the combustion temperature. This mixture is then expanded in the gas turbine. The mixture leaving the turbine is a major source of heat supply for the ORC. The second heat source is a mixture of steam and gas – a major supply of heat source for ORC. Next, the mixture is undergoing separation process in a cyclone separator and then the CO<sub>2</sub> (with a small content of moisture) is directed to carbon capture unit. The CO<sub>2</sub> is then compressed in a system that requires intercooling. Due to the wide range of temperatures of the listed waste heat sources, the double ORC combination is investigated. The combined ORC cycle is connected by a cascade heat exchanger. The ORC fluid parameters are selected computationally to match the temperature distribution lines. The power plant processes are simulated in the steady-state process simulator using the most accurate equations of state from the literature. Optimum operating conditions of the ORC integrated power plant are obtained through optimization techniques.

665

## 1 INTRODUCTION

The increasing demand for sustainable energy solutions has stimulated research into innovative ways of using waste heat to generate electricity. One such approach is the use of Organic Rankine Cycle (ORC) technology in conjunction with waste heat recovery from gasification or gas scrubbing processes in bioenergy with carbon capture and storage (BECCS) systems. This study deals with the modification of the thermodynamic cycle combining the negative CO<sub>2</sub> power plant concept with ORC. The investigated power plant operates with gas produced from the gasification of sewage sludge, where the negative emission term results from the aggregated CO<sub>2</sub> balance resulting from CO<sub>2</sub> capture. The introduction of ORC technology enables the utilisation of waste heat, ultimately increasing the overall efficiency of the power plant. In addition, research into multi-stage ORC combinations is addressing the wide range of temperatures associated with waste heat sources, paving the way for more advanced and efficient waste heat recovery systems.

Relevant literature includes work focusing on the integration of ORC technology and waste heat recovery in various applications. Mikielwicz et al., (2016) utilise waste heat from a power plant by employing a double-stage ORC system with bleed steam as heat source and an additional waste heat source from flue gas, thereby further improving energy efficiency. Moradi et al., (2020) investigate the feasibility of integrating biomass gasification with a steam-injected micro gas turbine and an ORC unit revealing that the ORC combination and steam injection into the combustion chamber results in higher net electrical power. Johansson et al., (2023) authors proposed a model that predicts convective and condensation heat recovery in a centrifugal scrubber, which may be applicable to gas scrubbing processes within BECCS systems. Brachi et al., (2022) explore the integration of waste heat recovery or ORC systems with sewage sludge gasification for combined heat and power (CHP) production in wastewater treatment plants, demonstrating improved energy efficiency and reduced environmental impact. Wang et al., (2021) investigate the integration of waste heat recovery using ORC technology with a counterflow direct contact scrubber for coal-fired flue gas treatment, demonstrating the simultaneous cleaning of the flue gas by removal of harmful pollutants and the recovery of waste heat for additional power generation through the ORC.

The process flow diagram (PFD) of negative emission CO<sub>2</sub> gas power plant (nCO<sub>2</sub>PP) is shown in Figure 1 (Ziółkowski et al., 2023). In this configuration, the GT<sup>bap</sup> turbine is used for the low pressure expansion. The novelty in the nCO<sub>2</sub>PP reference case presented in Ziółkowski et al., (2021) is the use of the Spray-Ejector Condenser (SEC) to condense the steam in a direct condensation process, separate the CO<sub>2</sub> and create the vacuum required by GT<sup>bap</sup>. There is also HE1, which cools the flue gases upstream of the SEC by regeneratively heating high pressure water fed to the Wet Combustion Chamber (WCC) (Ziółkowski et al., 2023).

The PFD, where ORC has been introduced instead of low pressure expansion, is shown in Figure 2. In this modification, the heat exchanger HE1 is located in the same place, but it receives energy from flue gases with a pressure of 1 bar and a significantly higher temperature. From an efficiency point of view, it is preferable that HE1 exchanges as much heat as possible. After HE1, an ORC cycle is incorporated to utilise the remaining heat that could not otherwise be used by HE1 but would be lost in the condenser. A second ORC stage is added to match the water condensation from the producer gas in the gas scrubber, where the temperature from the gasification unit is 760 °C. The flow from the first stage is also diverted for superheating to the temperature source, which is the main waste heat source of the second stage, this is done because the first stage has a higher pressure and therefore efficiency.

666

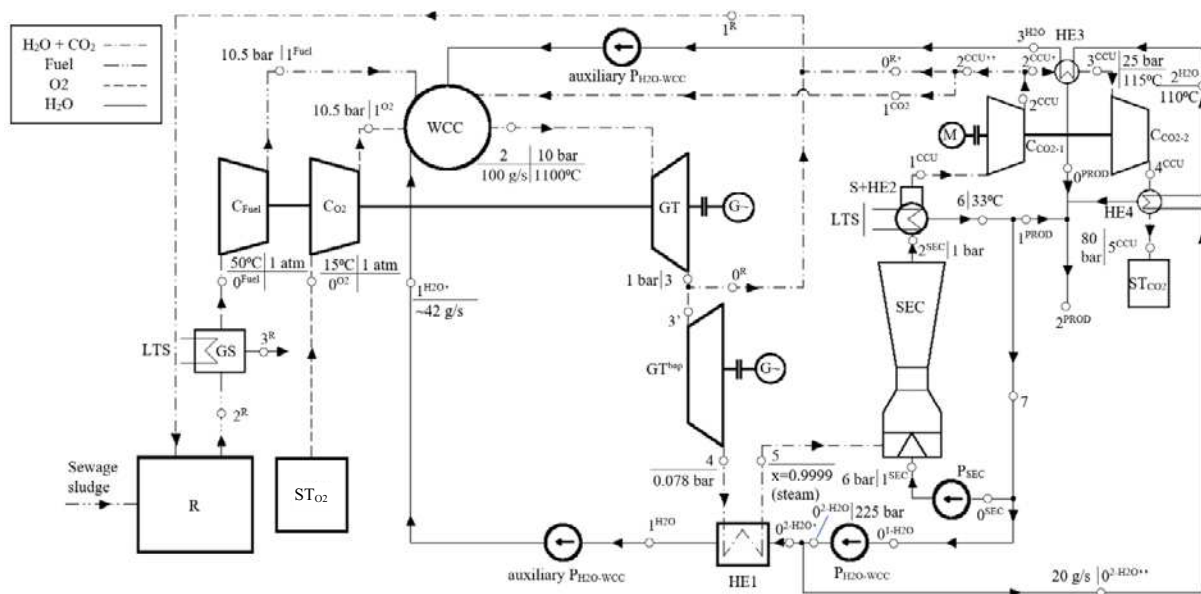


**Figure 1:** Process flow diagram of the negative CO<sub>2</sub> power plant reference case (Ziółkowski et al., 2023).

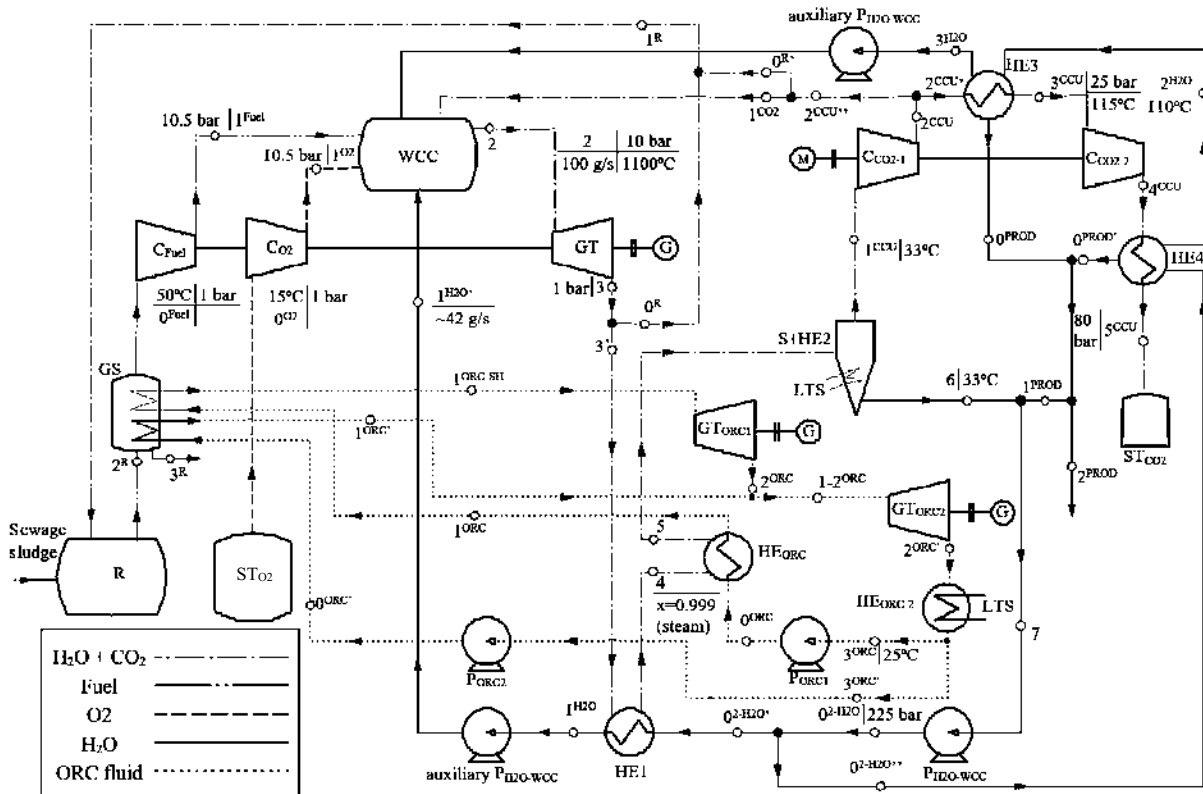


Figure 2: Process flow diagram of the negative CO<sub>2</sub> power plant with double stage ORC.

## 2 METHODOLOGY

The simulation software used in this study is Aspen Plus, which uses the REFPROP equations of state package, providing highly accurate calculations.

The ORC working fluid used in the simulation is R1233zd(E), which is a new promising candidate for industrial use in heat transfer applications due to its excellent thermodynamic properties, low price and low environmental impact (Pysz et al., 2023). Previously, the authors in Stasiak et al., (2022) conducted analyses of several ORC fluids and found R1233zd(E) to be the most favourable among them. In addition, R1233zd(E) is available for turbo chillers. This ORC fluid can be an alternative to R245fa and is therefore expected to be used for ORC.

For this study, the reference case nCO<sub>2</sub>PP (without ORC) is compared with its combination with one-stage ORC and with double-stage ORC.

The composition of sewage sludge digested in the gasification unit, was assumed as mass fractions 27.9% C, 6.7% H, 28.9% O, 4.4% N, 32.2% Ash, with an LHV of 9.8 MJ/kg (cf. Table 1) (Ziółkowski, Badur, et al., 2022). The efficiency of the gasifying reactor is  $\eta_{RH} = 0.71$  and HHV = 15.70 MJ/kg. The proximate and ultimate composition were taken from the work of Ziółkowski, Badur, et al., (2022).

The producer gas produced by gasification in a steam atmosphere at 760 °C and, after cleaning in the gas scrubber, has a volumetric composition of 9.3% CO, 46.8% H<sub>2</sub>, 13.9% CH<sub>4</sub>, 26.4% CO<sub>2</sub> and 3.5% C<sub>3</sub>H<sub>8</sub>. Assumptions for gas turbine equipment such as compressors, combustion chamber and expanders are given in Table 2. Among the most relevant parameters are the temperature of 1100 °C after the combustion chamber and the pressure of 10 bar. This work analysis was carried out for a commercial scale plant with a capacity of 10,000 tonnes of dried sewage sludge mass flow per year (see Table 2). The internal efficiencies of the GT/GT<sup>bap</sup> expanders, water pumps and compressors were assumed to be relatively high, but this was done to refer to previous work analysing the nCO<sub>2</sub>PP cycle (Ertesvåg et al., 2023; Stasiak et al., 2023; Ziółkowski, Głuch, et al., 2022). These values help to establish a reference value for two modifications of the system with ORC cycles.

**Table 1.** Proximate and ultimate analysis of sewage sludge for reactor (Ziółkowski, Badur, et al., 2022).

Specification	Unit	Value
Fixed Carbon	% <sub>dry</sub>	9.40
Volatile Matter	% <sub>dry</sub>	58.10
Ash	% <sub>dry</sub>	32.50
Moisture content *	% <sub>wb</sub>	2.00
C	% <sub>dry</sub>	27.89
H	% <sub>dry</sub>	6.67
N	% <sub>dry</sub>	4.36
S	% <sub>dry</sub>	0.29
O **	% <sub>dry</sub>	28.29

\* – assumed value, after drying of sewage sludge; \*\* – determined by difference

**Table 2.** Assumptions for the gas turbine cycle

Parameter	Symbol	Unit	Value
Temperature exhaust after WCC (before GT)	$t_2$	°C	1100
Mass flow of the dried sewage sludge mass flow annually	$\dot{m}_{ss}$	t/yr	10 000
Exhaust pressure after WCC	$p_2$	bar	10
Oxygen-fuel excess ratio in WCC	$\lambda$	-	1
Initial syngas temperature, after gas scrubber	$t_{fuel}$	°C	50
Initial oxygen temperature	$t_{O_2}$	°C	15
Syngas fuel pressure before $C_{fuel}$ compressor	$p_{0-fuel}$	bar	1
Oxygen pressure before $C_{O_2}$ compressor	$p_{0-O_2}$	bar	1
Fuel to WCC pressure loss factor	$\delta_{fuel}$	-	0.05
Oxygen to WCC pressure loss factor	$\delta_{O_2}$	-	0.05
Regenerative water pressure to WCC	$p_{1-H_2O}$	bar	225
Turbine GT, internal efficiency ( $\eta_i$ )	$\eta_{iGT}$	-	0.89
Turbine GT <sup>bap</sup> , $\eta_i$	$\eta_{iGT-bap}$	-	0.89
Fuel compressor $C_{fuel}$ , $\eta_i$	$\eta_{ic-fuel}$	-	0.87
Oxygen compressor $C_{O_2}$ , $\eta_i$	$\eta_{ic-O_2}$	-	0.87
WCC water pump $P_{H_2O-WCC}$ , $\eta_i$	$\eta_{iP-H_2O-WCC}$	-	0.8
Mechanical efficiency for all devices	$\eta_m$	-	0.99

The useful product in the GT/GT<sup>bap</sup> section is electricity. On the other hand, in the CCS unit with a set of compressors, the other desired product is the clean CO<sub>2</sub> obtained after the exhaust gas separation and subsequent compression. The assumptions for these units are given in Table 3.

Table 4 refers to the ORC cycle, where the useful product is electricity, but at the same time it is possible to compensate for the loss of waste heat energy to the environment. The basic assumptions for this new part of the system are the efficiencies of the pump, the expanders and the upper and lower temperatures in the evaporator and condenser. The internal efficiencies of the ORC turbines and the ORC pump were set at a high level for this type of equipment, namely 0.8 and 0.89 for the pump and the expanders, respectively (Micheli et al., 2013; Mikielwicz & Mikielwicz, 2010, 2014; Pan et al., 2020; Wajs et al., 2016). This is as reasonable as possible, given the potential of using hybrid algorithms to optimise flow systems (Delgado-Torres & Garcia-Rodríguez, 2010; Witanowski, Klonowicz, et al., 2023; Witanowski, Ziółkowski, et al., 2023; Zheng et al., 2023; Ziviani et al., 2014).

**Table 3.** Assumptions for CO<sub>2</sub> separation and CCS system.

Parameter	Symbol	Unit	Value
Exhaust vapor quality after HE1	$x_5$	-	0.999
Exhaust temperature after HE1, before SEC	$t_5$	°C	33
CO <sub>2</sub> pressure after compressor C <sub>CCU1</sub>	$p_{2-CCU}$	bar	25
CO <sub>2</sub> pressure after compressor C <sub>CCU2</sub>	$p_{4-CCU}$	bar	80
H <sub>2</sub> O temperature after HE4	$t_{2-H_2O}$	°C	110
CO <sub>2</sub> temperature after HE3	$t_{3-CCU}$	°C	115
Water vapor from Separator in 1 <sup>CCU</sup> mixed with CO <sub>2</sub> vapor	-	%	100% humid
Temperature after SEC	$t_6$	°C	35
SEC water pump P <sub>SEC</sub> , $\eta_i$	$\eta_{iP-SEC}$	-	0.8
CO <sub>2</sub> compressor C <sub>CO2-1</sub> , $\eta_i$	$\eta_{iC-CO2-1}$	-	0.87
CO <sub>2</sub> compressor C <sub>CO2-2</sub> , $\eta_i$	$\eta_{iC-CO2-2}$	-	0.87
Sewage sludge treated as renewable energy source by Polish law (MINISTERSTWO ŚRODOWISKA, 2016)	$R$	-	-0.9

**Table 4.** Assumptions for incorporation ORC

Parameter	Symbol	Unit	Value
Pressure after GT <sup>bap</sup> , without ORC	$p_4$	bar	0.078
Pressure after GT, when ORC is incorporated	$p_3$	bar	1
ORC lower temperature source	$t_{3-ORC}$	°C	25
ORC pump P <sub>ORC</sub> , $\eta_i$	$\eta_{iP-ORC}$	-	0.8
Turbine ORC-1, internal efficiency ( $\eta_i$ )	$\eta_{iT-ORC1}$	-	0.89
Turbine ORC-2, $\eta_i$	$\eta_{iT-ORC2}$	-	0.89

In addition, a paper Maksuta et al., (2017) presents a selection of examples of radial inflow and radial outflow ORC turbines with efficiencies of around 90% and outputs of the order of 3 MW. A paper Lampart et al., (2018) reports several ORC turbines with efficiencies as high as 89.6% at an inlet medium temperature of 175 °C. In another study available in the literature Zaniewski et al., (2019), one can find design and CFD calculations of turbines with proven efficiencies of 89-90% by both methods. These values refer to the radial inflow reaction turbine with a turbine inlet temperature of 210 °C. This type of design already has an established methodology in the world literature by experts in the field (Fiaschi et al., 2012).

Furthermore, in order to obtain optimal configurations of the flue gas heat recovery system, the thermodynamic cycles analysed in the literature start from a temperature difference of 3 K (Jankowski & Borsukiewicz, 2019). It is worth mentioning that the authors Jankowski & Borsukiewicz, (2019), as a result of comparing the two optimisation methods, obtained a similar optimal evaporation temperature in the evaporator for the refrigerant R1234yf, namely 85 °C. Similar values for the minimum temperature difference (namely 4 K) for an evaporator with an evaporation temperature of 140 °C were obtained by the authors Quoilin et al., (2011). On the other hand, in the context of heat recovery systems from low-temperature sources such as geothermal, the temperature difference in the exchanger is assumed to be 3-20 K (Liu et al., 2017). The authors Jankowski et al., (2020) carried out an optimisation for evaporation temperatures below 120 °C in ORC systems, achieving a minimum temperature difference of 5 K in the evaporator.

The economic analysis was carried out for a commercial scale plant with a capacity of 10,000 tonnes of dried sewage sludge mass flow per year (see Table 5), which could correspond to the capacity of a wastewater treatment plant. This scale plant is designed on the basis of commercial components (such as pumps, oxygen generation station, heat exchangers, etc.) and their operational reliability is high (they are guaranteed by their manufacturers). GT and GT<sup>bap</sup> with WCC and SEC, the sludge drying system and the gasifier with plasmatron are still prototypes, but will first be tested on a smaller scale.

**Table 5.** Assumptions for economic analysis

Parameter	Unit	Value
Two gas turbines with a combustor for nCO <sub>2</sub> PP reference case	EUR	-9 000 000
One gas turbine with a combustor for nCO <sub>2</sub> PP with ORC case	EUR	-6 000 000
Spray-ejector condenser, for nCO <sub>2</sub> PP reference case	EUR	-330 000
Spray-ejector condenser, for nCO <sub>2</sub> PP with ORC case	EUR	0
ORC one stage (1304 EUR per kW)	EUR	-796 265
ORC double stage (1304 EUR per kW)	EUR	-859 966
Auxiliary devices (Pumps, heat exchangers, CO <sub>2</sub> compressors)	EUR	-94 000
Plasma gasifier+ gas cleaning	EUR	-910 000
Pre-treatment (drying)	EUR	-980 000
Yearly cost of oxygen	EUR/yr	-1 369 236
Yearly cost of GT/GT <sup>bap</sup> servicing for nCO <sub>2</sub> PP reference case	EUR/yr	-900 000
Yearly cost of GT/GT <sup>bap</sup> servicing for nCO <sub>2</sub> PP with ORC case	EUR/yr	-600 000
Discount rate	%	6.9
Sewage sludge disposal price	EUR/t	53
Electricity price	EUR/MWh	311.2
Avoided CO <sub>2</sub> price	EUR/t	70

It is worth noting that the authors did not find an increase in efficiency but a decrease when using the additional heat source for ORC from the WCC. The decrease in efficiency of the whole system can be explained by the fact that a heat exchanger has to be used between the flue gas and the low boiling medium. Thus, the ORC medium entering the ORC cycle turbine is at least several degrees lower in temperature than the exhaust gas going directly from the WCC to the GT (see Figure 1). In addition, considering the present problem in terms of exergetic analysis, the addition of an exchanger instead of direct transfer of the medium to the expander results in entropy production and exergy destruction. Finally, in the methodology of this work it has been assumed that only waste heat (whereas in WCC it would not be waste heat), or improved heat management, is used for the ORC cycle, leaving the GT high pressure part as in the reference nCO<sub>2</sub>PP concept.

To illustrate the optimum choice of ORC parameters, Figure 3 shows a temperature distribution approach on a logarithmic scale for heat exchangers exchanging heat between the producer gas, the exhaust gas temperature lines and the ORC cooling fluid and pressurised water directed to the WCC temperature lines. This graph in Figure 3 is for one-stage ORC only, but this stage is the same as part of the double-stage ORC configuration, except for the superheat. The exhaust gas temperature is shown as a solid line, the ORC fluid as a dashed line and the pressurised water regeneratively heated by the hot waste heat exhaust gas before being fed to the WCC as a dotted line. In addition, the graph is divided into two segments, described at the top of the graph, where 'ORC' is the heat exchange taking place in the HE-ORC evaporator and 'HE1' corresponds to the heat exchange in the regenerative heat exchanger 'HE1' between the exhaust gas and the pressurised water fed to the WCC.



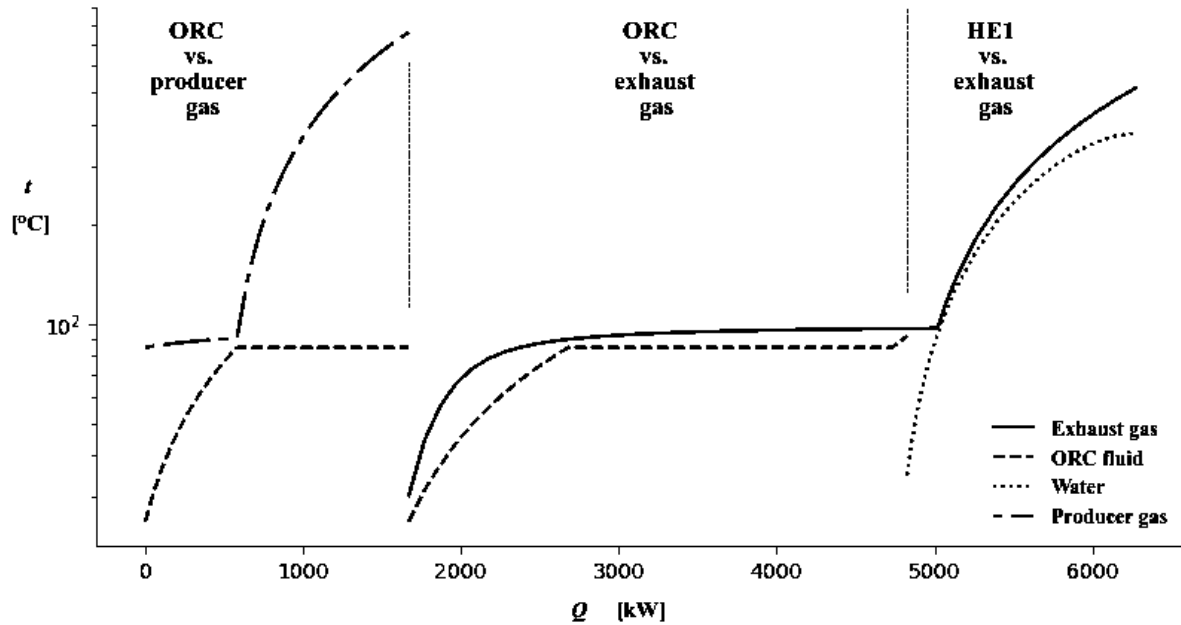


**Figure 3:** Logarithmic scale temperature distribution as ORC fluid in HE<sub>ORC</sub> and HE1 heat exchangers

## 2.1 Equations formulated

The net power (work rate):

$$\dot{W}_{net} = \dot{W}_t - \dot{W}_{cp} + \dot{W}_{t-ORC-1} + \dot{W}_{t-ORC-2} \quad (1)$$

where:  $\dot{W}_t$  is the power of the GT/GT<sup>bap</sup> gas turbines,  $\dot{W}_{cp}$  is the sum of the power consumption of the compressors and pumps,  $\dot{W}_{t-ORC-1}$  and  $\dot{W}_{t-ORC-2}$  are the power of the ORC turbines.

$$\begin{aligned} \dot{W}_{cp} = & \dot{W}_{C-Fuel} + \dot{W}_{C-O_2} + \dot{W}_{C-CO_2-1} + \dot{W}_{C-CO_2-2} + \dot{W}_{P-H_2O} + \dot{W}_{P-SEC} + \dot{W}_{P-ORC-1} \\ & + \dot{W}_{P-ORC-2} \end{aligned} \quad (2)$$

Where:  $\dot{W}_{C-Fuel}$ ,  $\dot{W}_{C-O_2}$ ,  $\dot{W}_{C-CO_2-1}$ ,  $\dot{W}_{C-CO_2-2}$  are compressor power consumption for fuel, oxygen, and carbon dioxide respectively, while  $\dot{W}_{P-H_2O}$ ,  $\dot{W}_{P-SEC}$  and  $\dot{W}_{P-ORC-1}$ ,  $\dot{W}_{P-ORC-2}$  are pump power consumption for WCC water supply, SEC water supply and ORC fluid drive, respectively.

The overall cumulative power plant efficiency:

$$\eta_{cum} = \eta_{RH} \cdot \frac{\dot{W}_{net}}{LHV_{syngas} \cdot \dot{m}_{0-fuel}} \quad (3)$$

Where  $\eta_{RH}$  is the hot gas efficiency of the gasifying reactor,  $LHV_{syngas}$  is the Lower Heating Value of the syngas and  $\dot{m}_{0-fuel}$  is the mass flow of the syngas.

The authors decided not to use the term net efficiency, which can be found in other works of the authors Ziółkowski et al., (2023), because it includes the efficiency of the gasification reactor, which is multiplied with the net efficiency of the whole nCO<sub>2</sub>PP system to form the cumulative efficiency and is therefore not called net efficiency, in order not to confuse both efficiency measures in their works. The CO<sub>2</sub> emissivity of the whole system is defined as follows:

$$eCO_2 = R \frac{\dot{m}_{2-CO_2}}{\dot{W}_{net}} 3600 \quad (4)$$

where  $\dot{m}_{2-CO_2}$  is the mass flow rate of CO<sub>2</sub> captured, R is the factor considered only for the power plant with the CO<sub>2</sub> capture, which indicates the fraction of the energy source that is treated as renewable by local law. If the system has CO<sub>2</sub> capture, the emission is zero, but if there is a renewable energy source, the value is negative. The avoided eCO<sub>2</sub> would be the sum of the emissions without CO<sub>2</sub> capture and an absolute value of the negative emissions from the renewable energy source.

The Net Present Value *NPV* is a widely used technique for the financial evaluation of long-term projects (Ziółkowski, Pawlak-kruczek, et al., 2022). It quantifies the surplus or deficit of cash flows in present value terms, reflecting the time value of money:

$$NPV = \sum_{t=1}^n \frac{CF_t}{(1+r)^t} - I_0 \quad (5)$$

where  $CF_t$  is the net cash flow in period  $t$ , while  $r$  is representative of the discount rate, and  $I_0$  stands for the initial investment. The variable  $t$  denotes the time at which the cash flow occurs, and  $n$  denotes the duration of the project. In addition to *NPV*, there is another important financial indicator - the internal rate of return (IRR). It is the discount rate that makes the *NPV* of all projected future cash flows equal to zero and serves as the break-even threshold, therefore it can be derived by finding the value of  $r$  in equation (5) that makes the *NPV* equal to zero.

It should be noted that the IRR assumes that cash flows are reinvested at the same rate, which may not be the reality for a long-term power plant project. Despite this limitation, the IRR remains a valuable measure of the potential profitability of a project.

The Levelized Cost of Electricity *LCOE* is another economic indicator that calculates the average cost of electricity production over the life of the project and is calculated according to BEIS (UK Department for Business, Energy & Industrial Strategy) (Aldersey-Williams & Rubert, 2019):

$$LCOE = \frac{\sum_{t=1}^n \frac{CF_{out,t}}{(1+r)^t}}{\sum_{t=1}^n \frac{E_t}{(1+r)^t}} \quad (6)$$

where  $CF_{out,t}$  is the capital cost in period  $t$  and  $E_t$  is the energy generated in period  $t$ , both being discounted. The *LCOE*, in this context, represents the net breakeven price per unit of total output (electricity plus other revenue streams per MWh), that a project must receive over its lifetime to cover all costs and break even. Therefore a lower *LCOE* indicates a more economically competitive project. In addition, the *LCOE* often decreases as the lifetime of a project increases, as the costs are spread over a larger volume of electricity produced.

### 3 RESULTS AND DISCUSSION

Table 6 shows the main results for the two ORC cycle variants with the pressures of the individual ORC pumps and the upper temperatures. In the one-stage ORC variant the ORC fluid is saturated (84.8 °C) (see Figure 4), while in the double-stage variant it is superheated (171.7 °C) (see Figure 5), both at a pressure of 7.38 bar. Also in the double-stage variant, the ORC flow is injected at a lower pressure (5.24 bar) between two turbines with a saturated temperature of 72.6 °C. Figure 4 shows a temperature distribution plot on a logarithmic scale for heat exchangers in one-stage ORC configuration exchanging heat between the exhaust gas temperature line and the ORC cooling fluid and pressurised water directed to the WCC temperature lines. Figure 5 shows the double-stage variant.



**Table 6.** Results for the ORC power cycle (both layout) with pressure, temperature, mass flow rate for the relevant cases.

nCO <sub>2</sub> PP case	$\dot{m}_{ORC}$ , g/s	$p_{ORC1}$ , bar	$p_{ORC2}$ , bar	$t_{ORC-SH}$ , °C	$t_{ORC}$ , °C
one-stage ORC	20,965	7.38	-	84.8	-
double-stage ORC	19,012	7.38	5.24	171.7	72.6

Table 7 shows the results comparing different nCO<sub>2</sub>PP cases. First is the reference case nCO<sub>2</sub>PP power plant with SEC and no ORC (Ziółkowski et al., 2023), then the hybrid nCO<sub>2</sub>PP with one-stage ORC using R1233zd(E) refrigerant as working fluid, and then the double-stage ORC. One-stage ORC differs from double-stage ORC in that only one ORC boiling temperature is used. In addition, each result corresponds to the maximum overall net power plant efficiency obtained by adjusting the optimum ORC parameters, namely ORC boiling temperature and mass flow. For comparison, the CO<sub>2</sub> mass flow in the flue gas, the total mechanical power of the turbines, the power for own consumption, the chemical energy rate from combustion, the cumulative efficiency of the nCO<sub>2</sub>PP power plant are shown, the emisivity and the avoided CO<sub>2</sub> emissions are shown.

**Table 7:** Different configurations results

nCO <sub>2</sub> PP case	$\dot{m}_{2-CO_2}$ , g/s	$\dot{W}_T$ , kW	$\dot{W}_{cp}$ , kW	$\dot{Q}_{CC}$ , kW	$\eta_{cum}$ , %	$eCO_2$ , kgCO <sub>2</sub> /MWh	Avoid $eCO_2$ , kgCO <sub>2</sub> /MWh
reference (Ziółkowski et al., 2023)	313	2,107	602	3,785	27.9	-672.8	1,420.3
one-stage ORC	313	2,120	376	3,813	32.3	-580	1,224.4
double-stage ORC	313	2,167	374	3,813	33.2	-551.3	1,163.8

673

It can be seen that the cumulative efficiency is increased compared to the reference case. The main reason for this is that in the reference case there is a low pressure expansion obtained by the spray ejector condenser, which is driven by a pump with high electricity consumption to move a large amount of water. The low pressure expansion also allows a higher gas turbine output. In the ORC combination cases, there is no low pressure expansion, but the ORC is treated as a moisture exhaust gas condenser, recovering waste heat from this process, thus increasing the amount of waste heat recovered water that goes to the WCC, further increasing the water content in the exhaust gas. In addition, in ORC variants, water from the producer gas is condensed in the gas scrubber. The first stage operates at a higher boiling point, with a pressure of 7.38 bar and a mass flow of 13,301 g/s (see Figure 5), allowing it to effectively recover heat from the flue gas water condensation. Meanwhile, the second stage is designed to match the producer gas water condensation in the gas scrubber, with the ORC fluid pressure maintained at 5.24 bar and 5,714 g/s mass flow. The higher temperature of the producer gas is used to overheat the working fluid in the first stage, as the increased pressure of the working fluid in this stage results in higher efficiency. For comparison purposes, a one-stage ORC has been configured (see Figure 4), and for this purpose the efficiency of this configuration is the maximum, where the ORC fluid also recovers heat from the producer gas at the gasification temperature of 760 °C and pressure of 1 bar (which gradually condenses water below 90.6 °C), but is not able to use all the waste heat because it is a single stage adapted to a different temperature source at 96.8 °C and 1 bar pressure (which gradually condenses water below this temperature). There are two main reasons for the increased efficiency of the double-stage ORC compared to the one-stage ORC, although in both the one-stage and the double-stage ORC the parameters are optimised for maximum efficiency. The first is that the additional stage fits better to the temperature line of the producer gas during moisture condensation, thus recovering more heat in the lower temperature region, and then, to maximise efficiency, the remaining heat at 760 °C from the producer gas is used to overheat the higher boiling temperature ORC stage. The secondary small increase from the addition of the second ORC stage is due to the connection of the second stage turbine,

which reduces entropy generation. The main reason for this is that mixing the expanded working fluid with the additional flow effectively lowers the average temperature of the mixture, thereby reducing the entropy generated during the expansion process. When the mixed fluid enters the second turbine, it expands at a lower average temperature and the entropy generated at this stage is also lower than in a one-stage turbine. The emissivity (as well as its avoided variant), which is negative for all nCO<sub>2</sub>PP cases, decreases in its absolute values for the ORC cases, which is a positive trend, meaning that less CO<sub>2</sub> would be emitted into the environment if it was not captured. It also means that a higher power output is obtained for the same amount of CO<sub>2</sub> flow in the system.

Table 8 compares the economic results of three scenarios over a decade: a reference case and two ORC variants using either a one-stage or a double-stage ORC. From a financial perspective, the double-stage ORC outperforms the other two, with the highest IRR and NPV, implying the highest profits. In addition, the double-stage ORC gives the lowest LCOE, which means it is the most cost-effective in terms of electricity production (plus other revenue streams per MWh). Therefore, the double-stage ORC scenario appears to be the most economically advantageous.

**Table 8:** Results for economic analysis for 10 year lifetime

nCO <sub>2</sub> PP case	$\dot{m}_{SS}$ , t/yr	$\dot{m}_{CO_2}$ , t/yr	$E_t$ , MWh/yr	IRR, %	NPV, EUR	LCOE, EUR/MWh
reference (Ziółkowski et al., 2023)	10,000	9,854	13,191	27.8	11,876,698	276
one-stage ORC	10,000	9,854	15,277	48.5	20,565,106	200
double-stage ORC	10,000	9,854	15,707	49.7	21,445,389	195

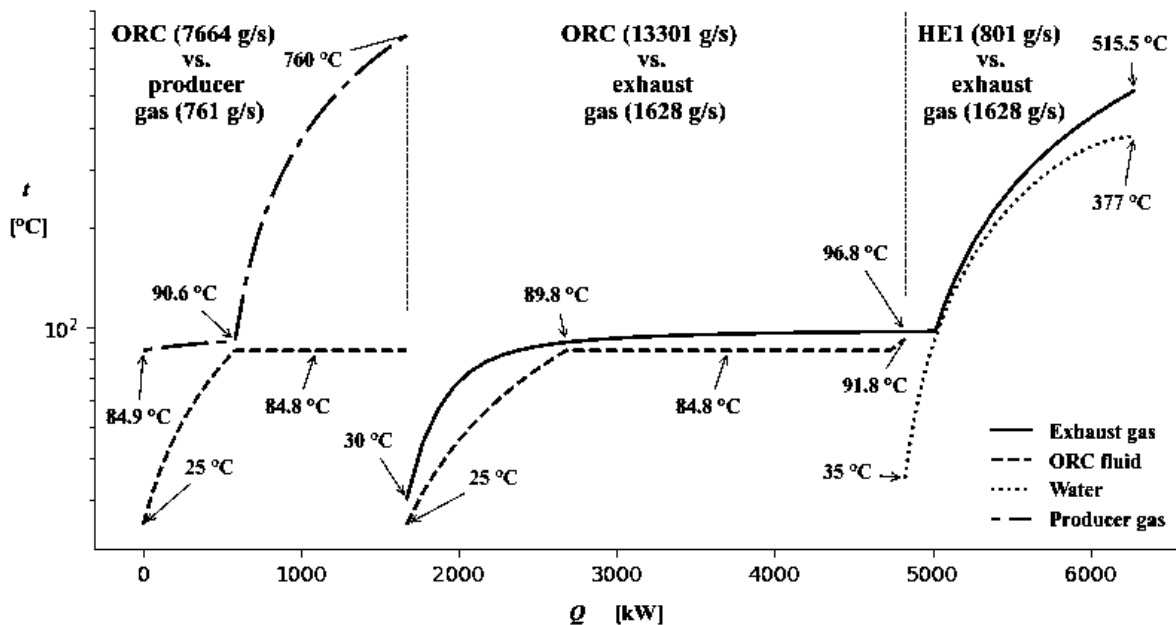


**Figure 4:** Logarithmic scale temperature distribution with R1233zd(E) as ORC fluid in one-stage HE<sub>ORC</sub> and HE1 heat exchangers

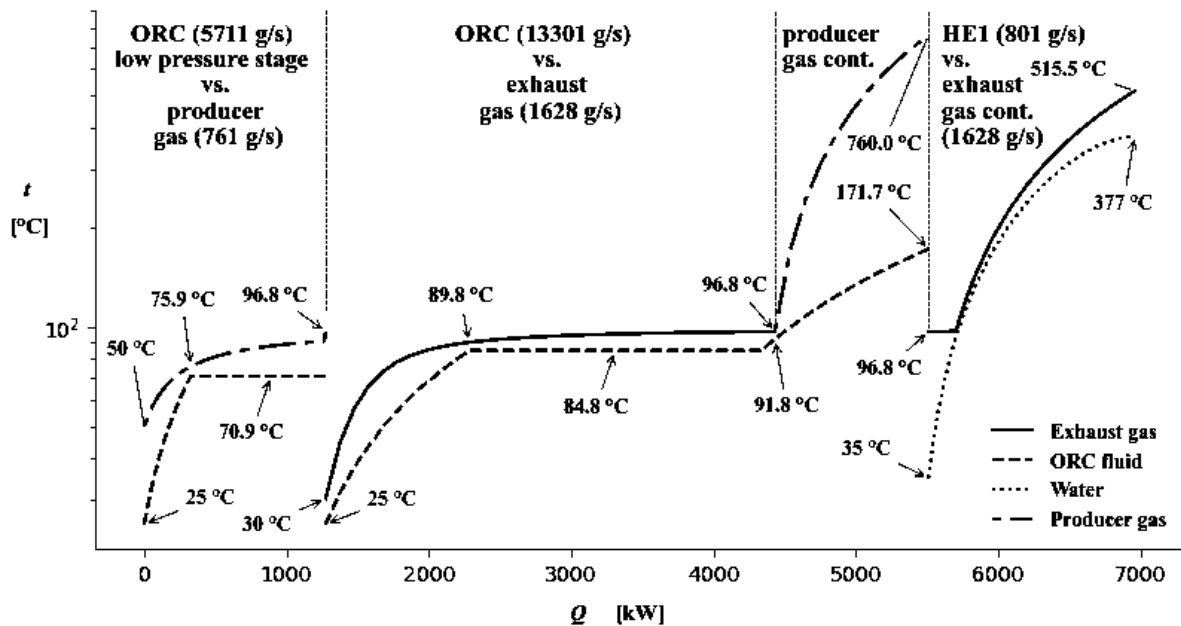


**Figure 5:** Logarithmic scale temperature distribution with R1233zd(E) as ORC fluid in double-stage  $HE_{ORC}$  and HE1 heat exchangers

## 4 CONCLUSIONS

The integration of a double-stage ORC using R1233zd(E) as the working fluid significantly improves the cumulative efficiency of the  $nCO_2PP$  power plant (33.2%) compared to a one-stage ORC (32.3%) or the reference case (27.9%). The ORC integration has an efficiency advantage over the reference case due to the increased heat recovery and the elimination of the high power spray ejector pump. However, the double-stage ORC has an advantage over the one-stage ORC due to better adaptation to the second temperature source. Another reason is the reduction in entropy generation due to the addition of the lower temperature ORC fluid flow to the first stage expanded flow prior to the second turbine expansion. By using an advanced heat recovery process of a double-stage ORC combined with the  $nCO_2PP$  power plant and exploiting the special thermodynamic properties of R1233zd(E), this conceptual configuration achieved the highest efficiency.

The results suggest that the implementation of ORC in the negative  $CO_2$  emission system outperforms the reference case in terms of energy efficiency, economic return and environmental benefits. The double-stage ORC offers a moderate increase in efficiency and economic return when considering the trade-off in complexity compared to the one-stage ORC variant. Double-stage also offers the lowest  $CO_2$  emissivity in absolute terms, resulting in less  $CO_2$  emissions to mitigate, which is consistent with sustainable and economically sound practices driven by revenue streams.

## Nomenclature

$eCO_2$	emissivity of $CO_2$ , $kgCO_2/MWh$
$\dot{m}$	mass flow rate, g/s
$N$	power, kW
$p$	pressure, bar
$t$	temperature, °C

## Greek symbols

$\eta_{cum}$	cumulative efficiency, %
$\eta_i$	internal efficiency of devices, %

$\eta_m$	mechanical efficiency of devices, %
$\eta_{RH}$	gasifying reactor efficiency, %
<b>Abbreviations</b>	
BECCS	bioenergy with carbon capture and storage
C	compressor
CCS	carbon capture and storage
G	generator
GS	gas scrubber
GT	gas turbine
HE	heat exchanger
IRR	internal rate of return
LCOE	levelised cost of electricity
nCO <sub>2</sub> PP	negative CO <sub>2</sub> emission gas power plant
NPV	net present value
P	pump
R	gasifier
SEC	spray ejector condenser
WCC	wet combustion chamber

## REFERENCES

- Aldersey-Williams, J., & Rubert, T. (2019). Levelised cost of energy – A theoretical justification and critical assessment. *Energy Policy*, 124, 169–179. <https://doi.org/10.1016/j.enpol.2018.10.004>
- Brachi, P., Di Fraia, S., Massarotti, N., & Vanoli, L. (2022). Combined heat and power production based on sewage sludge gasification: An energy-efficient solution for wastewater treatment plants. *Energy Conversion and Management: X*, 13, 100171. <https://doi.org/10.1016/J.ECMX.2021.100171>
- Delgado-Torres, A. M., & García-Rodríguez, L. (2010). Analysis and optimization of the low-temperature solar organic Rankine cycle (ORC). *Energy Conversion and Management*, 51(12), 2846–2856. <https://doi.org/10.1016/j.enconman.2010.06.022>
- Ertesvåg, I. S., Madejski, P., Ziółkowski, P., & Mikielewicz, D. (2023). Exergy analysis of a negative CO<sub>2</sub> emission gas power plant based on water oxy-combustion of syngas from sewage sludge gasification and CCS. *Energy*, 278, 127690. <https://doi.org/10.1016/J.ENERGY.2023.127690>
- Fiaschi, D., Manfrida, G., & Maraschiello, F. (2012). Thermo-fluid dynamics preliminary design of turbo-expanders for ORC cycles. *Applied Energy*, 97, 601–608. <https://doi.org/10.1016/j.apenergy.2012.02.033>
- Jankowski, M., & Borsukiewicz, A. (2019). Multi-objective approach for determination of optimal operating parameters in low-temperature ORC power plant. *Energy Conversion and Management*, 200, 112075. <https://doi.org/10.1016/j.enconman.2019.112075>
- Jankowski, M., Borsukiewicz, A., Wiśniewski, S., & Hooman, K. (2020). Multi-objective analysis of an influence of a geothermal water salinity on optimal operating parameters in low-temperature ORC power plant. *Energy*, 202, 117666. <https://doi.org/10.1016/j.energy.2020.117666>
- Johansson, W., Li, J., & Lin, L. (2023). Module-based simulation model for prediction of convective and condensational heat recovery in a centrifugal wet scrubber. *Applied Thermal Engineering*, 219, 119454. <https://doi.org/10.1016/J.APPLTHERMALENG.2022.119454>
- Lampart, P., Witanowski, Ł., & Klonowicz, P. (2018). Efficiency Optimisation of Blade Shape in Steam and ORC Turbines. *Mechanics and Mechanical Engineering*, 22(2), 553–564. <https://doi.org/10.2478/mme-2018-0044>
- Liu, X., Zhang, Y., & Shen, J. (2017). System performance optimization of ORC-based geo-plant with R245fa under different geothermal water inlet temperatures. *Geothermics*, 66, 134–142. <https://doi.org/10.1016/j.geothermics.2016.12.004>

- Maksiuta, D., Moroz, L., Burlaka, M., & Govoruschenko, Y. (2017). Study on applicability of radial-outflow turbine type for 3 MW WHR organic Rankine cycle. *Energy Procedia*, 129, 293–300. <https://doi.org/10.1016/J.EGYPRO.2017.09.156>
- Micheli, D., Pinamonti, P., Reini, M., & Taccani, R. (2013). Performance Analysis and Working Fluid Optimization of a Cogenerative Organic Rankine Cycle Plant. *Journal of Energy Resources Technology, Transactions of the ASME*, 135(2). <https://doi.org/10.1115/1.4023098/365899>
- Mikielewicz, D., & Mikielewicz, J. (2010). A thermodynamic criterion for selection of working fluid for subcritical and supercritical domestic micro CHP. *Applied Thermal Engineering*, 30(16), 2357–2362. <https://doi.org/10.1016/j.applthermaleng.2010.05.035>
- Mikielewicz, D., & Mikielewicz, J. (2014). Analytical method for calculation of heat source temperature drop for the Organic Rankine Cycle application. *Applied Thermal Engineering*, 63(2), 541–550. <https://doi.org/10.1016/j.applthermaleng.2013.11.047>
- Mikielewicz, D., Wajs, J., Ziółkowski, P., & Mikielewicz, J. (2016). Utilisation of waste heat from the power plant by use of the ORC aided with bleed steam and extra source of heat. *Energy*, 97, 11–19. <https://doi.org/10.1016/j.energy.2015.12.106>
- MINISTERSTWO ŚRODOWISKA. (2016). *Dziennik ustaw Rozporządzenie Ministra środowiska w sprawie warunków technicznych kwalifikowania części energii odzyskanej z termicznego przekształcania odpadów*. <https://isap.sejm.gov.pl/isap.nsf/download.xsp/WDU20160000847/O/D20160847.pdf>
- Moradi, R., Marcantonio, V., Cioccolanti, L., & Bocci, E. (2020). Integrating biomass gasification with a steam-injected micro gas turbine and an Organic Rankine Cycle unit for combined heat and power production. *Energy Conversion and Management*, 205, 112464. <https://doi.org/10.1016/J.ENCONMAN.2019.112464>
- Pan, Z., Yan, M., Shang, L., Li, P., Zhang, L., & Liu, J. (2020). Thermoeconomic analysis of a combined natural gas cogeneration system with a supercritical CO<sub>2</sub> brayton cycle and an organic rankine cycle. *Journal of Energy Resources Technology, Transactions of the ASME*, 142(10). <https://doi.org/10.1115/1.4047306/1083973>
- Pysz, M., Głuch, S., & Mikielewicz, D. (2023). Experimental study of flow boiling pressure drop and heat transfer of R1233zd(E) at moderate and high saturation temperatures. *International Journal of Heat and Mass Transfer*, 204, 123855. <https://doi.org/10.1016/J.IJHEATMASSTRANSFER.2023.123855>
- Quoilin, S., Declaye, S., Tchanche, B. F., & Lemort, V. (2011). Thermo-economic optimization of waste heat recovery Organic Rankine Cycles. *Applied Thermal Engineering*, 31(14–15), 2885–2893. <https://doi.org/10.1016/j.applthermaleng.2011.05.014>
- Stasiak, K., Ertesvåg, I. S., Ziółkowski, P., & Mikielewicz, D. (2023). Exergetic analysis of the nCO<sub>2</sub>PP cycle with particular reference to the exergy destruction of sewage sludge due to gasification. *THE 36TH INTERNATIONAL CONFERENCE ON EFFICIENCY, COST, OPTIMIZATION, SIMULATION AND ENVIRONMENTAL IMPACT OF ENERGY SYSTEMS*.
- Stasiak, K., Ziółkowski, P., & Mikielewicz, D. (2022). Assessment, optimisation and working fluid comparison of organic Rankine cycle combined with negative CO<sub>2</sub> gas power plant system. *7th International Conference on Contemporary Problems of Thermal Engineering*, 357–367. [https://www.s-conferences.eu/ftp/cpote/CPOTE\\_proceedings\\_19\\_10.pdf](https://www.s-conferences.eu/ftp/cpote/CPOTE_proceedings_19_10.pdf)
- Wajs, J., Mikielewicz, D., Bajor, M., & Kneba, Z. (2016). Experimental investigation of domestic micro-CHP based on the gas boiler fitted with ORC module. *Archives of Thermodynamics*, 37(3), 79–93. <https://doi.org/10.1515/AOTER-2016-0021>
- Wang, H., Wu, X., Liu, Z., Granlund, K., Lahdelma, R., Li, J., Teppo, E., Yu, L., Duamu, L., Li, X., & Haavisto, I. (2021). Waste heat recovery mechanism for coal-fired flue gas in a counter-flow direct contact scrubber. *Energy*, 237, 121531. <https://doi.org/10.1016/J.ENERGY.2021.121531>
- Witanowski, Ł., Klonowicz, P., Lampart, P., & Ziółkowski, P. (2023). Multi-objective optimization of the ORC axial turbine for a waste heat recovery system working in two modes: cogeneration and condensation. *Energy*, 264, 126187. <https://doi.org/10.1016/j.energy.2022.126187>

- Witanowski, Ł., Ziółkowski, P., Klonowicz, P., & Lampart, P. (2023). A hybrid approach to optimization of radial inflow turbine with principal component analysis. *Energy*, 272, 127064. <https://doi.org/10.1016/j.energy.2023.127064>
- Zaniewski, D., Klimaszewski, P., Witanowski, Ł., Jędrzejewski, Ł., Klonowicz, P., & Lampart, P. (2019). Comparison of an impulse and a reaction turbine stage for an ORC power plant. *Archives of Thermodynamics*.
- Zheng, J., Zhong, J., Chen, M., & He, K. (2023). A reinforced hybrid genetic algorithm for the traveling salesman problem. *Computers & Operations Research*, 157, 106249. <https://doi.org/10.1016/j.cor.2023.106249>
- Ziółkowski, P., Badur, J., Pawlak-Kruczek, H., Stasiak, K., Amiri, M., Niedzwiecki, L., Krochmalny, K., Mularski, J., Madejski, P., & Mikielwicz, D. (2022). Mathematical modelling of gasification process of sewage sludge in reactor of negative CO<sub>2</sub> emission power plant. *Energy*, 244. <https://doi.org/10.1016/j.energy.2021.122601>
- Ziółkowski, P., Głuch, S., Ziółkowski, P. J., & Badur, J. (2022). Compact High Efficiency and Zero-Emission Gas-Fired Power Plant with Oxy-Combustion and Carbon Capture. *Energies*, 15(7), 2590. <https://doi.org/10.3390/en15072590>
- Ziółkowski, P., Madejski, P., Amiri, M., Kuś, T., Stasiak, K., Subramanian, N., Pawlak-Kruczek, H., Badur, J., Niedzwiecki, Ł., & Mikielwicz, D. (2021). Thermodynamic analysis of negative CO<sub>2</sub> emission power plant using aspen plus, aspen Hysys, and ebsilon software. *Energies*, 14(19). <https://doi.org/10.3390/en14196304>
- Ziółkowski, P., Pawlak-kruczek, H., Madejski, P., Bukowski, P., Ochrymiuk, T., Stasiak, K., Amiri, M., Niedzwiecki, L., & Mikielwicz, D. (2022). Thermodynamic, ecological, and economic analysis of negative CO<sub>2</sub> emission power plant using gasified sewage sludge. *2nd International Conference on Negative CO<sub>2</sub> Emissions*.
- Ziółkowski, P., Stasiak, K., Amiri, M., & Mikielwicz, D. (2023). Negative carbon dioxide gas power plant integrated with gasification of sewage sludge. *Energy*, 262, 125496. <https://doi.org/10.1016/j.energy.2022.125496>
- Ziviani, D., Beyene, A., & Venturini, M. (2014). Design, Analysis and Optimization of a Micro-CHP System Based on Organic Rankine Cycle for Ultralow Grade Thermal Energy Recovery. *Journal of Energy Resources Technology*, 136(1). <https://doi.org/10.1115/1.4024858>

### ACKNOWLEDGEMENT

The research leading to these results has been funded by Norway Grants 2014-2021 via the National Centre for Research and Development. This study has been prepared within the project "Negative CO<sub>2</sub> Emission Gas Power Plant" - NOR/POLNORCCS/NEGATIVE-CO<sub>2</sub>-PP/0009/2019-00, co-funded by the "Applied Research" Programme under the Norwegian Financial Mechanisms 2014-2021 POLNOR CCS 2019 - Development of CO<sub>2</sub> capture solutions integrated in power and industrial processes.